4-25-2021

Identification and Analysis of Massive Galaxies with High Star Formation Rate

Andrew Guillory

Identification and Analysis of Massive Galaxies with High Star Formation Rate

by

Andrew Guillory

An Honors Capstone

submitted in partial fulfillment of the requirements

for the Honors Certificate

to

The Honors College

of

The University of Alabama in Huntsville

4/25/2021

Honors Capstone Director: Dr. Ming Sun

Associate Professor of Astrophysics

Andrew Guillory 4/25/2021
Student Date

Ming Sun 04/26/2021
Director Date

JAM Digitally signed by James Miller
DN: cn=James Miller, o=UAH, ou=PH & ISEd, email=millerja@uah.edu, c=US
Date: 2021.04.29 14:26:05 -05'00'
Department Chair Date

William Wilkerson Digitally signed by William Wilkerson
Date: 2021.05.02 17:43:40 -05'00'
Honors College Dean Date

Honors College
Frank Franz Hall
+1 (256) 824-6450 (voice)
+1 (256) 824-7339 (fax)
honors@uah.edu

Honors Thesis Copyright Permission

This form must be signed by the student and submitted as a bound part of the thesis.

In presenting this thesis in partial fulfillment of the requirements for Honors Diploma or Certificate from The University of Alabama in Huntsville, I agree that the Library of this University shall make it freely available for inspection. I further agree that permission for extensive copying for scholarly purposes may be granted by my advisor or, in his/her absence, by the Chair of the Department, Director of the Program, or the Dean of the Honors College. It is also understood that due recognition shall be given to me and to The University of Alabama in Huntsville in any scholarly use which may be made of any material in this thesis.

__Andrew Guillory_____________

Student Name (printed)

Andrew Guillory
____

Student Signature

_4/25/2021__

Date

Table of Contents

Abstract:

This research project focuses on the use of online astronomical databases to identify massive galaxies with high star formation rates (SFR). The primary database used was the GSWLC collaborative catalog to gather a sample of galaxies that included the galaxies' mass, UV and IR spectrums, and their SFR predicted by these respective spectrums. Using graphical analysis of the carefully selected data set, we were able to identify significant bounds and relationships to galaxy mass and SFR. Some in depth analysis of a few smaller subsets of galaxies was also performed to find extreme examples of galaxies with high SFR.

Background:

Before looking at the process of performing this research, it is important to establish some context for why this project was important. This section will provide some background on the significance of studying SFRs of galaxies and a look at the various astronomy databases used to for this research.

Studying Star Formation Rate

Studying SFR of galaxies is an important part of understanding how they grow and evolve. It helps us to better understand how gas and dust molecules filter throughout the galaxy. We can estimate SFR through theoretical models by analyzing how individual stars grow based on various factors such as gas concentrations, the size of the star, or even if the star is located inside a star cluster. With these factors, and many others, in mind we can calculate how stars can grow into different sizes and have extremely different lifespans. We can observe that galaxies with high SFRs will typically boast higher populations of massive hot blue stars. By looking at how the different materials within a galaxy are distributed through the Initial Mass Function (IMF) it is noted that galaxies with high SFR will create more high mass stars and thus have a luminosity distribution that favors high energy light, such as UV. Along with this, though, the galaxy will also create many more low mass stars. For reference, consider a star created in a galaxy with mass M. For every star created in this galaxy of mass M there will be roughly 2.5 times as many stars with mass M/2 (this can vary based on the model of the IMF you use) [2]. This may not seem like a lot but when you consider that the Milky Way galaxy contains about 10^{11} stars then these factors start to show their influence. Even though there are many more low mass stars created during high periods of SFR in a galaxy, high mass stars will have much brighter luminosities and will thus contribute to the overall luminosity function of the galaxy more significantly. As another quick reference for this scale, a star that is 100 solar masses will have a luminosity about 1 million times that of the Sun (a single solar mass). Thus, we can tell that galaxies with high SFR will form more high mass stars and thus emit more high energy radiation than galaxies that are stagnant or not in a period of high star formation.

With these conclusions, astronomers have found that we can identify galaxies with high SFR and estimate its value based on the bolometric luminosity of certain wavelengths of light from the galaxy. If we can see that a galaxy is emitting high amounts of UV radiation, then we can use this to estimate its SFR. There are many different methods for estimating SFR based on luminosity calibrations, but most of these rely heavily on the accuracy of the IMF being used and the time frame being explored for the period of high SFR. This type of analysis can also be done with other wavelengths of light, as well. An even more difficult endeavor is estimating the SFR of a galaxy based on the infrared (IR) emissions. While IR radiation is certainly of a much lower energy compared to UV emissions, they are still significant in searching for galaxies with high

SFR. High IR radiation from galaxies can many times indicate large amounts of hot interstellar dust that has been heated by the stars around it. Dust will absorb the energy from the stars around it and then re-release the energy as IR radiation. Thus, if a galaxy has high amounts of IR radiation it could be an indicator that the galaxy has many hot stars within it that we do not observe UV radiation coming from since it is being scattered by dust [1]. Galaxies with high dust attenuation will typically not have as significant star formation since higher dust counts indicates that it has gone through many phases of star populations. Thus, much of its material has been cycled through many high mass stars to disperse more dust into the interstellar medium. Still, older galaxies can have periods of star formation and are thus worth studying. While not explored in this paper, comparing galaxies with high IR radiation to galaxies with high UV radiation can help to understand how different amounts of dust can affect the overall luminosity output of the galaxy.

Catalogs and Databases

Moving on from the theoretical discussion, this section will explore the different sources of empirical data that we can use to explore and analyze the topic of SFR. For this project, we focused primarily on one main catalog: GALEX-SDSS-WISE Legacy Catalog (GSWLC). This database is a collaboration of three different databases that is attempting to create a more comprehensive singular catalog. So far, GSWLC contains combined spectroscopic data on about 700,000 different galaxies [3]. Included in this data is estimates in SFR based on UV and IR spectrum. While there is still a significant amount of data that needs to be added, this catalog has already proved to be an extremely useful source and is thus the primary database used in this research project. To better understand the complexity of this database, a brief description of the collaborated catalogs is given here.

Starting with the first letter in the GSWLC acronym, the Galaxy Evolution Explorer (GALEX) is a space telescope dedicated to surveying galaxies in UV light. It was launched in 2003 and was in service until 2012. It surveyed about 77% of the sky in near UV and far UV light, and observations were led by teams at California Technical Institute [4]. It boasted incredibly sensitive instruments that gave it capabilities of observing extremely distant galaxies. Having UV emission data on various galaxies also gives empirical data to test against theoretical estimates. Its observations are used in the GSWLC catalog to help provide SFR estimates based on UV emissions.

The next database is the Sloan Digital Sky Survey (SDSS). This is a less specialize database compared to the other two catalogs included in GSWLC. This database intends to be a full comprehensive mapping of the entire sky. This project started in 1998 and continues to grow to this day [5]. It contains imaging data on an incredible number of points and partners with other databases to create a more complete imaging of the sky. As of right now, SDSS has accurately mapped approximately one quarter of the entire sky [5]. The drawback of this massive imaging survey is that it does not contain detailed data on most of its recorded points. Some points in the massive database do contain more in-depth spectroscopic data which is usually provided by other databases that focus on creating surveys of specific attributes on a smaller sample of objects. However, despite the many collaborations helping with completing SDSS, there are many objects that do not have any spectroscopic data and only contain imaging and positional data. Still, the sheer number of objects that it has mapped and cataloged has made SDSS one of the most invaluable astronomy resources to date. It makes searching for large groups of objects a much easier task than ever before, and it is especially useful for collaborative databases, such as the GSWLC.

The last database included in the GSWLC is the Wide-field Infrared Survey Explorer, or WISE. This, as the name suggests, is another satellite telescope that surveys the sky in a few different IR bands. The four main IR wavelengths used in this catalog are: 3.4, 4.6, 12, and 22 μm [6]. The satellite was launched in 2009 with the mission of creating a full sky survey across these IR bands. During its approximately one-year active-duty phase, WISE was able to complete its mission and resulted in a source catalog of over 200 million points with positional and spectroscopic data. An all-sky IR survey is important for a variety of reasons, but, for the sake of the GSWLC catalog, it is essential to observing distant active galaxies that have active IR spectrum. By observing the sky in IR radiation, we can observe distant galaxies that would usually be obscured by dust clouds that lie within the line of sight between us and a galaxy. This is significant as dust clouds will typically absorb and scatter higher energy light such as UV and optical [7]. IR emissions will, however, pass through. This allows us to see through dust clouds and observe distant galaxies that have high IR spectrums. As we stated before, this is an important part in analyzing galaxies with potentially high SFR.

With this context in mind, we continue to the primary subject: identifying high SFR galaxies.

Data collection:

To begin the analysis, it was necessary to decide on the set of data that would be used for the project. Looking at the GSWLC website [3], there are three primary data sets that are offered: A, D, and M. The A-table is the largest table with the most points but has limited data and accuracy for each point in the data set. The D-table is the second largest and contains more in depth and reliable data on each point. The M-table is the most detailed table for each point but is the smallest table and only covers a handle full of points. With these different elements in mind, the A-table was chosen as the primary data set. This table contains data on about 640,000 points. Starting off with a large data sample is advantageous in this case as it allows for a higher chance of finding objects that fit with our specifications. Once we can establish constraints for the data then we can narrow down the sample and perform further analysis on the points that match these constraints.

One of the best ways to analyze large sets of data is by using graph analysis. Attempting to analyze 600,000 individual points is a monolithic task that is hardly practical. Graph analysis allows for an easy method of establishing trends amongst large groups of data and makes it easy to see where extreme examples may lie. This is also important to finding upper and lower bounds for SFR and masses of the galaxies. Figures 1 and 2 show the first two plots that were generated based on the data. Both were generated using the Matplotlib library in Python which has a variety of tools for analyzing these types of graphs [8].

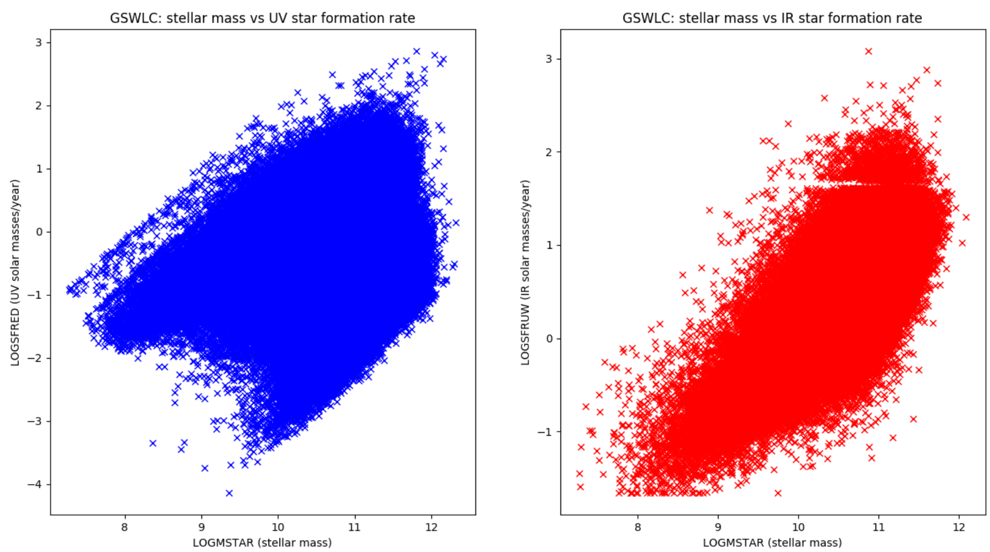

<u>Figure 1 (left):</u> Scatter plot of UV estimated SFR in solar masses per year vs the total mass of each galaxy measured in solar masses. <u>Figure 2 (right):</u> Scatter plot of IR estimated SFR in solar masses per year vs the total mass of each galaxy measured in solar masses. Both axes for each graph are measured in logarithmic scale.

These plots were standard scatter plots that were generated to give a baseline for what we could expect our further analysis to follow. While these graphs do look like massive blobs of randomly plotted points, they do allow for a good starting point as they are already showing us some trends and bounds in the data. For example, from Figure 1, we can see the highest UV estimated SFR is just below a magnitude of 3. From Figure 2, the highest IR estimated SFR is around a 3 magnitude as well with just one point lying directly above. The upper mass limit for both graphs is around 12. Along with these maximums, we can also see some an interesting trend forming between SFR and mass. However, to continue, different graphs will be required. While the point graphs are useful as an initial start, a new method of graphing will be more intuitive.

A few different graphing methods were considered. To start, we considered graphing a smaller sample of points and seeing if the graph would end up less cluttered and easier to read. However, this process would be unnecessarily tedious as we would need to find some method for what points would be excluded. Plus, this would run the risk of leaving out significant points at the extreme ends of the graph. Thus, it was decided that scatter plots were not the best method for our next set of graphs. Instead, new graphs were generated as density plots, or, more specifically, Kernel Density Estimate (KDE) plots. This would create a graph that is more akin to a heat map and would show where there is a high density of points based on SFR and mass. This was achieved by using another Python library named Seaborn [9]. These plots are shown in Figures 3 and 4.

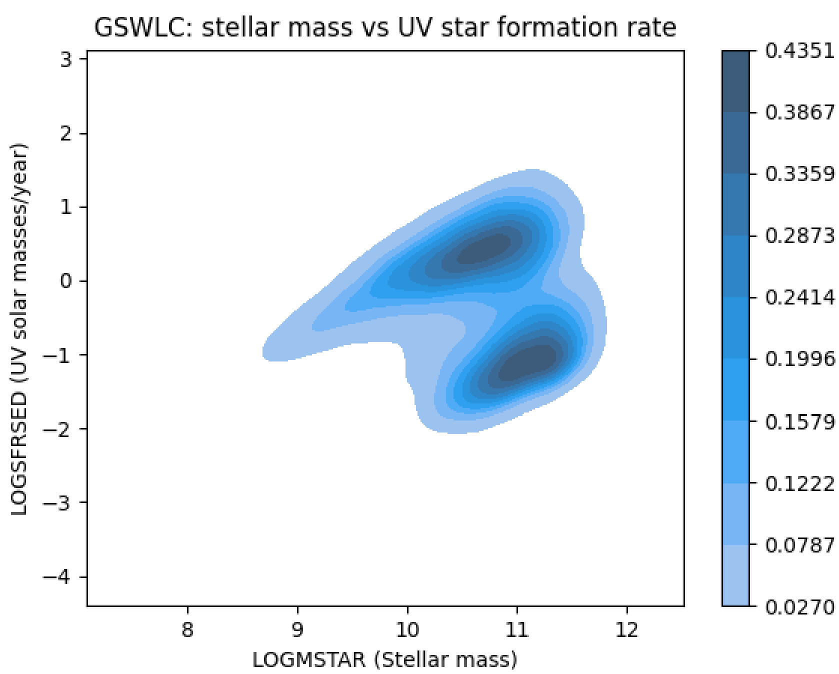

Figure 3: Density plot of UV estimated SFR vs total stellar mass of each galaxy. The darker regions of the plot indicate areas of higher density as given by the scale on the left side. This was the result of approximately 600,000 data points.

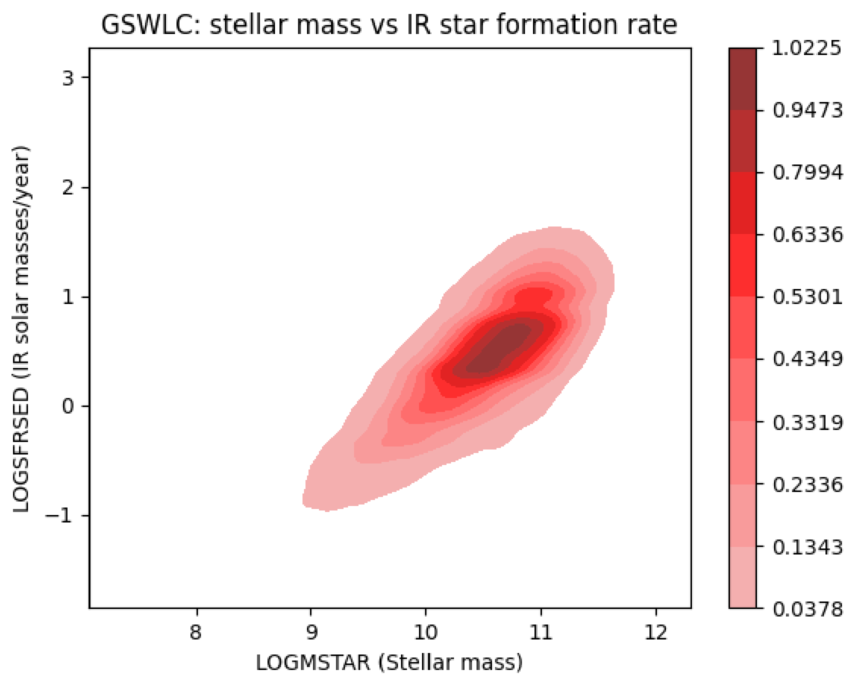

Figure 4: Density plot of IR estimated SFR vs total stellar mass of each galaxy. The darker regions of the plot indicate areas of higher density as given by the scale on the left side. This was the result of plotting approximately 200,000 data points.

These two plots give a bit more information as to the distribution of the data. Figure 3 shows two significant groupings of data. One density group lies at SFR magnitude of around 0.7 and a mass magnitude of ~10.8. The other grouping is around 1.2 SFR and a mass magnitude of ~11. Figure 4, which graphs the IR SFR against mass, has only a single grouping that greatly resembles the top grouping in Figure 3. This is interesting to see as it can potentially indicate that SFR estimates between UV and IR are fairly accurate. We can also see the similar maximum values in the density plots as we did from the scatter plots.

Something worth noting is that the IR distribution would potentially look exactly like the UV distribution, and have two significant high-density groups, if the IR data in the A-table was more complete. Most of the 640,000 points within the A-table had reliable UV data whereas only about a third of the table had reliable IR data. There were many instances where the estimated SFR based on IR was labelled with -99 which indicated that no reliable data was available. This also occurred with a hand full of UV data but not as significant in amount as the IR data. Python was used to filter these points out so that they would not skew the density plots.

One last plot that is worth looking into was another density plot but this time graphing UV SFR against the IR SFR (Figure 5). This graph is useful to see how the two estimates relate to each other. The graph shows there is a mostly linear correlation with some scattering along the

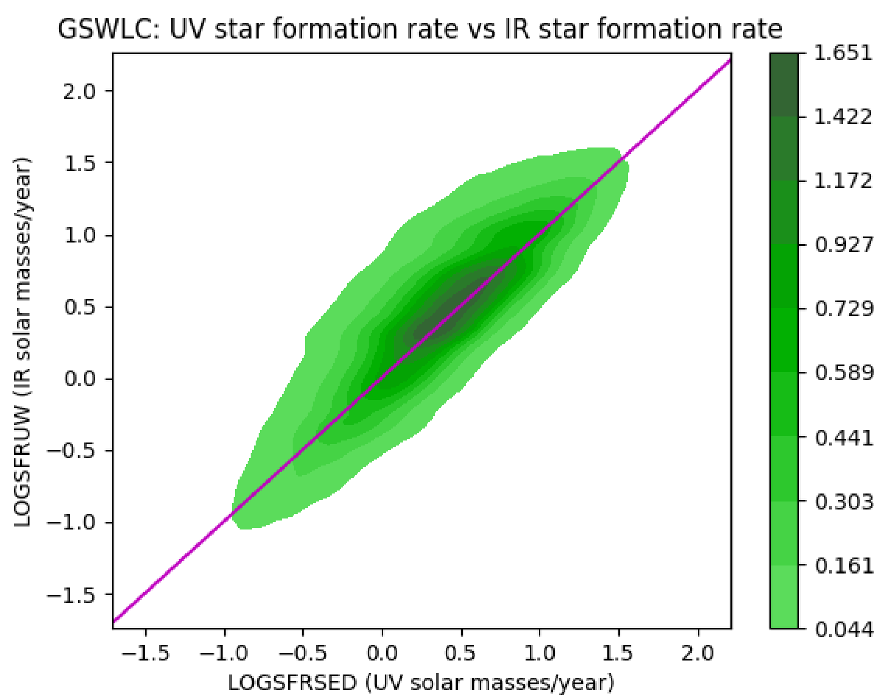

Figure 5: Another KDE graph plotting UV SFR vs IR SFR. An equality line of y=x is also superimposed for easier correlation analysis. This was done for most of the 200,000 reliable IR data points.

equality line (the magenta line through the middle). This tight correlation is good as it shows that the estimates for SFR are relatively consistent when estimating based on different wavelengths. Another interesting take away from this graph is the high density grouping with SFR magnitude of 0.5 on both axes. This shows that we can reasonably expect potentially active galaxies to have a SFR around this value. One last noteworthy point from this graph is the maximum SFR which lies just above 1.5 for the UV and IR estimates. This is good to check for consistency throughout each analysis, and the similar cutoff values for both axes is another promising correlation.

Applying Constraints

The graphing analysis was useful step to understanding overall trends in the data. The next step is to establish some constraints for analyzing subsets that have high mass and high SFR. This was done through two trial constraints that generated two different subsets of data.

Initial Constraints

As a starting point for the initial constraints, the upper bounds found in the graphs were used. We defined the SFR constraint as a point having greater than 50 solar masses per year which is approximately a 1.7 magnitude. The mass constraint was set to an 11.8 magnitude. A Python script (Figure 6) was used to filter the data set based on these constraints.

```
for i in range(t):

    #output string to text document
    #includes: ObjID, ra, dec, redshift, mass, UV SFR, IR SFR
    instr = str(OBJID[i]) + " " + str(RA[i]) + " " + str(DECL[i]) + " " + str(Z[i]) + " " + str(LOGMSTAR[i]) +

    #check if the galaxy has high mass
    if float(LOGMSTAR[i]) >= 11.8:


        #check if the galaxy has high UV star formation rate
        if float(LOGSFRSED[i]) >= 1.7:

            UV_out.write(instr)
            potential_UV = potential_UV +1


            Pos_out.write(str(RA[i]) + " " + str(DECL[i]) + "\n")


        #check if the galaxy has high IR star formation rate
        if float(LOGSFRUW[i]) >= 1.7:

            IR_out.write(instr)
            potential_IR = potential_IR +1


            Pos_out.write("**\n" + str(RA[i]) + " " + str(DECL[i]) + "\n**\n")
```

Figure 6: Sample Python 3 code for filtering the data based on constraints. This shows constraints based on the initial constraints. This same code sample was slightly modified for second set of constraints.

These constraints resulted in a subset of 16 data points. The script above checks both the UV and IR SFR estimates and will chose the point if it has a magnitude equal to or greater than the SFR constraint. Of the 16 points, 15 were selected due to the UV SFR meeting the constraints and only one was chosen for the IR SFR estimate. As mentioned before, the IR data in GSWLC is not as complete as the UV data so lack of reliable IR points could be attributed to this. Upon analyzing this data set, it was found that only about half of the points were robust data points that warranted further analysis. Most of the points were omitted due to bad image observation which was typically due to something in the foreground (i.e. a star or another galaxy) in the image that obscured the object. Others were also omitted due to having unreliable flux values for UV and IR which would have been used for further estimate checking of the SFR values. This data sample is shown in Table 1.

Table 1: Data set generated from initial constraints. Red highlight indicates omitted points.						
RA	DECL	Z	Log mass	Log UV SFR	Log IR SFR	Selected based on
194.53267	1.582208	0.1597	12.151	2.733	-99	UV
210.25863	2.878466	0.252	11.888	2.446	1.172	UV
121.0142	40.802595	0.1262	11.849	1.16	1.736	IR
3.609146	-0.110417	0.2324	11.808	2.857	-99	UV
167.84849	43.912804	0.1457	11.81	2.243	-99	UV
186.23115	41.962094	0.2495	11.822	1.715	1.346	UV
233.37967	7.732663	0.2124	11.91	1.733	-99	UV
327.1521	0.560117	0.2938	11.867	1.705	-99	UV
11.676815	0.116701	0.2763	11.913	2.573	-99	UV
152.52936	32.891407	0.2899	11.885	1.755	-99	UV
225.09492	22.007609	0.2141	11.848	1.804	-99	UV
175.03611	29.489528	0.2542	12.116	2.67	-99	UV
128.1299	13.407153	0.2777	11.816	1.798	-99	UV
164.88988	18.030032	0.2683	11.913	2.352	-99	UV
37.798679	1.25776	0.2699	12.038	2.799	-99	UV

Refining Constraints

Some of the points in the first table appear promising but, due to the lack of many reliable points from this dataset, it was decided that the analysis could be better if new constraints were considered. The new constraints would need to be a bit more inclusive while still giving a reliable data set with more extreme examples. The new constraints were to keep the mass of the galaxies the same at an 11.8 magnitude but greatly reduce the SFR down to 10 solar masses per year (1 magnitude) and introduce a new constraint of a redshift, z, of less than 0.1. There were, unfortunately, no galaxies that matched these constraints. After some trial and error, new conditions were settled on with a mass magnitude of at least 11.6, SFR of at least 5 solar masses per year (~0.7 magnitude), and z<0.1. After adjusting the conditions in the code in Figure 6, the data sample generated resulted in 18 points with all of them having good UV data and 7 of them also having good IR data. This proved to be a much more promising set than the table generated by the first constraints. No points were omitted as they all had good imaging and most had good flux data as well. This data set is shown in Table 2.

Table 2: Data set generated by refined constraints

RA	DECL	Z	Log mass	Log UV SFR	Log IR SFR	Selected based on
185.36089	-3.219796	0.0934	11.674	0.961	0.831	UV and IR
154.80727	59.131076	0.0725	11.749	0.72	-99	UV
202.79596	-1.727312	0.0835	11.647	0.991	1.04	UV and IR
139.27513	48.57478	0.0799	11.664	1.082	0.785	UV and IR
179.04304	60.522543	0.0332	11.63	1.034	1.289	UV and IR
179.84598	13.287794	0.0817	11.77	0.827	-99	UV
186.25118	40.157327	0.0736	11.614	1.105	0.579	UV
204.05602	10.478204	0.0538	11.6	0.768	0.503	UV
221.46529	36.145375	0.0988	11.648	0.778	1.031	UV and IR
217.3007	12.860888	0.0792	11.728	0.939	0.69	UV
130.20621	62.164598	0.0691	11.607	1.11	0.817	UV and IR
218.07063	33.590714	0.0847	11.634	0.83	0.542	UV
240.90419	20.954287	0.0869	11.621	0.728	0.546	UV
196.30899	31.999724	0.0519	11.683	0.747	1.388	UV and IR
179.76458	30.114501	0.0798	11.677	0.708	0.16	UV
146.22351	22.885116	0.089	11.842	0.86	0.751	UV and IR
136.16753	17.420222	0.0925	11.747	0.981	0.826	UV and IR

Since each constraint was modified in some way from their original values, it is difficult to pinpoint exactly why this data set appears to be more reliable. However, it is reasonable to assume that the redshift constraint had no small part in deciding these points. It is easier to obtain data on galaxies that are closer to us in the universe than those that are further away. It is worth noting, though, that the maximum SFR listed in Table 2 is 1.11 whereas all the points in Table 1 have higher SFR estimates than this. So, while the new data set is more reliable, it is lacking in more extreme examples, but does make up for this by also having reliable IR data for all its points. The original plan for this research project was to do more in depth analysis of the data by estimating the SFR values ourselves. Unfortunately, due to time constraints, this part of the research was not completed.

Results

While the final part of this project was omitted, there are still important results to be considered from the subsets generated from the constraints imposed on the data. By comparing Table 1 and Table 2, galaxies with a lower redshift will consistently have lower SFR. Despite the limited sample size, this is consistent with current predictions as well. It is expected that galaxies at larger redshifts go through more periods of SFR since we are observing them when they were relatively young. From the final data set of the final constraint values, two points were analyzed. These are shown in Figures 7 and 8.


Figure 7 (left): Spiral galaxy with position ra = 179.04304 and dec = 60.522543. This galaxy also has the designation of NGC 3978. Figure 8 (right): An elliptical galaxy (the most central point) appears to be apart of a system of three galaxies near each other. It has position ra = 202.79596 and dec = -1.727312. Both galaxies were identified in the sample defined by the final constraints.

Figure 7 is of particular interest as it is galaxy that would be expected to have high SFR. Bright blue spiral galaxies tend to have high concentrations of hydrogen in its interstellar medium and cycles materials at a relatively rapid rate compared to other galaxy types. It is interesting in terms of the data set as it has high UV and IR SFR estimates. Many of the other points show impressive SFR based either UV or IR estimates so seeing a point that has high SFR based on both estimates could be worth more investigation. This could be especially useful to find more information on the dust attenuation within the galaxy and how that effects UV and IR emissions for a younger galaxy. The other galaxy, noted in Figure 8, also lies on the upper end of the SFR estimates within this sample. This is interesting to see as the galaxy appears to be elliptical which we typically expect to have lower SFR compared to other galaxy types. It is possible that it is going through a period of SFR, but it is also likely, given that it has neighbors in proximity, that it is on the verge of merging with the other galaxies and the exchanging of material has sparked a new stage of increased star formation. It is difficult to say for sure without analyzing the other galaxies and without figuring out their exact distances from each other, but this is an interesting case that could be worth researching further to see the effects on SFR for galaxies that could potentially merge.

Apart from the constraint samples, the graphical analysis also gave useful upper bounds for the SFRs, and mass ranges where we can reasonably expect to have galaxies with high star formation activity. We also found that our SFR estimates correlate well based on the density plot comparing UV and IR SFRs. As mentioned earlier, however, this analysis could be skewed due to the incompleteness of the IR data in the GSWLC catalog.

Conclusions

SFR is an important topic in astronomy and is critical to understanding the overall evolution of galaxies. By studying SFR estimates we can see various correlations by other characteristics of galaxies and from how galaxies may interact with each other. From this project we can conclude that current SFR estimates are fairly accurate, but more analysis and data collection can help to improve our understanding, especially with IR data. Future research could expand on this project by using other databases with potentially more complete IR data. Further analyzing the WISE source catalog could be a good starting point for continuing research. Analyzing the UV and IR flux values of the galaxy samples can also provide a way to empirically check current SFR estimates and analyze possible adjustments. Testing different constraints is an important part of seeing the effects of SFR. As seen in this project, the redshift of a galaxy seemed to greatly effect the expected SFR we might see from it so researching other characteristics of galaxies could lead to other useful trends.

Star formation rate of massive galaxies is an important topic that still requires more research to fully understand. Understanding the extreme examples of data sets like the ones presented here can allow for a better understanding into these difficult topics.

Acknowledgements

I would like to give special thanks to the University of Alabama in Huntsville for there many research opportunities. I would also like to thank David Cook, Nichole Hughes, and all the other faculty involved in the Honors College that support the various undergraduate research programs. I would like to show appreciation to the UAH Physics department and all the faculty members who are always ready to give help and encourage students to pursue physics and science. One last special thanks I would like to give is to Dr. Ming Sun. I have been fortunate enough to have worked on a few different research projects under his mentorship since my second year of college. His willingness to continue advising and teaching me has helped me to become a better researcher and academic. I am incredibly thankful to have had him for an advisor.

Bibliography

1. Calzetti, Daniela. *Star Formation Rate Indicators - Daniela Calzetti*, California Technical Institute, ned.ipac.caltech.edu/level5/Sept12/Calzetti/Calzetti1_2.html.

2. *Encyclopedia of Astronomy and Astrophysics- Galaxy Evolution.* Institute of Physics Publishing, 2001.

3. "GSWLC." *GSWLC (GALEX-SDSS-WISE LEGACY CATALOG)*, salims.pages.iu.edu/gswlc/.

4. "Overview." *GALEX*, www.galex.caltech.edu/about/overview.html.

5. "What Is the Sloan Digital Sky Survey?" *SDSS SkyServer DR16*, skyserver.sdss.org/dr16/en/sdss/sdsshome.aspx.

6. "The Wide-field Infrared Survey Explorer at IPACWISE" *All-Sky Data Release*, California Technical Institute, wise2.ipac.caltech.edu/docs/release/allsky/.

7. "Science Overview." *WISE*, UCLA and JPL, wise.ssl.berkeley.edu/science.html.

8. "Visualization with Python." Matplotlib, matplotlib.org/.

9. "Statistical Data Visualization." *Seaborn*, seaborn.pydata.org/.